

Sampling methodologies and dosage assessment techniques for submicrometre and ultrafine virus aerosol particles

C.J. Hogan Jr^{1,2}, E.M. Kettleison^{1,2}, M.-H. Lee^{1,2}, B. Ramaswami², L.T. Angenent^{2,3} and P. Biswas^{1,2,3}

¹Aerosol and Air Quality Research Laboratory, ²Environmental Engineering Science Program and ³Department of Chemical Engineering, Washington University in St Louis, St Louis, MO, USA

2005/0258: received 10 March 2005, revised 21 May 2005 and accepted 22 May 2005

ABSTRACT

C.J. HOGAN JR, E.M. KETTLEISON, M.-H. LEE, B. RAMASWAMI, L.T. ANGENENT AND P. BISWAS. 2005.

Aims: The aerosolization and collection of submicrometre and ultrafine virus particles were studied with the objective of developing robust and accurate methodologies to study airborne viruses.

Methods and Results: The collection efficiencies of three sampling devices used to sample airborne biological particles – the All Glass Impinger 30, the SKC BioSampler® and a frit bubbler – were evaluated for submicrometre and ultrafine virus particles. Test virus aerosol particles were produced by atomizing suspensions of single-stranded RNA and double-stranded DNA bacteriophages. Size distribution results show that the fraction of viruses present in typical aqueous virus suspensions is extremely low such that the presence of viruses has little effect on the particle size distribution of atomized suspensions. It has been found that none of the tested samplers are adequate in collecting submicrometre and ultrafine virus particles, with collection efficiencies for all samplers below 10% in the 30–100 nm size range. Plaque assays and particle counting measurements showed that all tested samplers have time-varying virus particle collection efficiencies. A method to determine the size distribution function of viable virus containing particles utilizing differential mobility selection was also developed.

Conclusions: A combination of differential mobility analysis and traditional plaque assay techniques can be used to fully characterize airborne viruses.

Significance and Impact of the Study: The data and methods presented here provide a fundamental basis for future studies of submicrometre and ultrafine airborne virus particles.

Keywords: aerosol sampling, biological nanoparticles, differential mobility analysis, dosage, virus aerosols.

INTRODUCTION

Airborne viruses, such as poxviruses and influenza, are of particular concern because of their ability for rapid infection via the respiratory system. Most viruses are on the order of 25–400 nm (Madigan *et al.* 1997) in characteristic length, and are known to associate with larger particles and aggregate in natural systems (Hull *et al.* 1970; Hirst and Pons 1973; Aller *et al.* 2005). This will lead to a virus particle (defined as a particle containing at least one virus)

size distribution which spans the ultrafine (<100 nm), submicrometre (<1 µm) and micrometre (>1 µm) size ranges. Airborne virus particle size distributions are rarely reported, and the samplers commonly used to collect virus particles have been designed for the collection of micrometre-sized particles (Grinshpun *et al.* 1997; Willeke *et al.* 1998). Therefore, previous virus aerosol studies using such samplers were limited to the study of micrometre-sized particles (Trouwborst and Kuyper 1974; Trouwborst *et al.* 1974; Ijaz *et al.* 1994; Brooks *et al.* 2005; Tseng and Li 2005). However, it is unknown as to whether the majority of virus particles in the ambient air are in the micrometre size range, or if a substantial fraction of virus particles are in the submicrometre and ultrafine size ranges. Submicrometre

Correspondence to: Pratim Biswas, Department of Chemical Engineering, Box 1180, Washington University in St Louis, St Louis, MO 63130, USA (e-mail: pratim.biswas@wustl.edu).

and ultrafine particles containing viable viruses would be particularly harmful because of the ability of particles in these size ranges to diffuse through alveolar membranes and rapidly enter the blood stream. Recent research has shown that the size of inhaled particles greatly determines the toxicological and immunological effects the particles have, and in general, the effects are much greater for submicrometre and ultrafine particles (Cassee *et al.* 2002; Esmen *et al.* 2002; Daigle *et al.* 2003). Therefore, knowledge of the size distribution of airborne virus particles in ambient studies and control of the size distribution of aerosolized virus particles in laboratory studies are of the utmost importance because the health effects of inhaled particles are particle size dependent.

For laboratory scale evaluation and animal respiratory challenges, biological aerosols have been aerosolized almost exclusively using collision nebulizers (Ijaz *et al.* 1994; Lin *et al.* 2000; Agranovski *et al.* 2002; Bray *et al.* 2002; Mainelis *et al.* 2002a; Tseng and Li 2005). However, most virus propagation media foam during the nebulization process, thus additional sample preparation, such as dialysis or centrifugation, is usually required in order to use collision nebulizers to aerosolize biological particles.

Airborne biological particles have traditionally been sampled using liquid impingers, which rely on inertial collection mechanisms to collect particles (Terzieva *et al.* 1996; Tseng and Li 2005). Liquid impingers have a distinct advantage in the collection of biological particles in that most biological analyses require samples contained in liquid media (Terzieva *et al.* 1996; Lin *et al.* 2000). In many commercial impingers, sampling liquid loss through evaporation and the reaerosolization of collected particles greatly reduces the collection efficiency and viability of particles (Lin *et al.* 1997, 1999, 2000). The SKC BioSampler® (SKC Inc., Eighty Four, PA, USA), also called the swirling aerosol collector, was designed by Willeke *et al.* (1998) to prevent the loss of sampling liquid during operation and to prevent damage to bacterial cells during collection. It, along with other commercial impingers, has been characterized with regard to the collection of airborne bacterial cells and spores (Lin *et al.* 1999, 2000). Despite full-scale evaluation for the collection of micrometre-sized particles, to the best of our knowledge, the physical collection efficiency of liquid impingers has not been evaluated for ultrafine and submicrometre particles with diameters <300 nm.

Here, the aerosolization of submicrometre and ultrafine virus particles and subsequent collection in three samplers which utilize liquid impingement are evaluated. The aerosolization method used is similar to that used in respiratory challenges (Roy *et al.* 2003a,b; Roy and Hartings 2003). The collection efficiency of the All Glass Impinger 30 (ACE Glass Inc., Vineland, NJ, USA), the SKC BioSampler®,

and a frit bubbler (ACE Glass Inc.) for submicrometre and ultrafine particles is examined as a function of particle size, sampler flow rate, and sampling time, using single-stranded RNA (ssRNA) and double-stranded DNA (dsDNA) bacteriophages as test viruses. The size distributions of aerosolized virus suspensions are presented with discussion on methods to control virus particle size distributions. As many studies use the aforementioned samplers, a strategy to estimate the correction factors necessary to find the true airborne virus concentration (or airborne virus dosage) is provided. A method utilizing differential mobility selection to determine the size distribution function of particles which contain viable viruses is also developed and used on the aerosolized virus suspensions in this study. Overall, this study provides a fundamental background for future studies of submicrometre and ultrafine airborne virus particles.

MATERIALS AND METHODS

Virus suspensions

Bacteriophages MS2 (ATCC 15597-B1) and T3 (ATCC 11303-B3) were used as test viruses in this study. MS2 bacteriophage is an ssRNA icosahedral virus. A single virion has an approximate diameter of 27.5 nm (Golmohammadi *et al.* 1993). T3 is a multi-subunit dsDNA virus with a small tail subunit and a spherical head that is approx. 45 nm in diameter. MS2 bacteriophages were propagated in bacterial host *Escherichia coli* (ATCC 15597) in a glucose and thiamine minimal media to a titre of 2×10^{10} PFU ml⁻¹. For aerosolization, filtered stock suspensions of MS2 were diluted with filtered deionized water (Milli-Q Ultrapure Water Purification System; Millipore, Billerica, MA, USA) to a titre of 5×10^9 PFU ml⁻¹. T3 bacteriophage stock suspensions were prepared in a similar fashion using bacterial host *E. coli* (ATCC 11303) in an LB broth, calcium chloride and magnesium sulfate solution. The filtered and diluted T3 suspension had a titre of 2.3×10^8 PFU ml⁻¹.

Liquid impingement samplers

We evaluated the virus particle collection efficiency of three different samplers, the All Glass Impinger 30 (AGI-30), the SKC BioSampler® and a frit bubbler. Drawings of the samplers are shown in Fig. 1. All three samplers utilize a collecting liquid to capture and retain aerosol particles. Aerosol particles enter the AGI-30 and flow through a 1 mm diameter nozzle, which is 30 mm above the base of the impinger. When filled with 20 ml of liquid, the nozzle outlet is 10 mm above the resting liquid surface. The sampler outlet is above the nozzle outlet, thus there is a sharp turn in flow streamlines at the nozzle outlet, just above the liquid

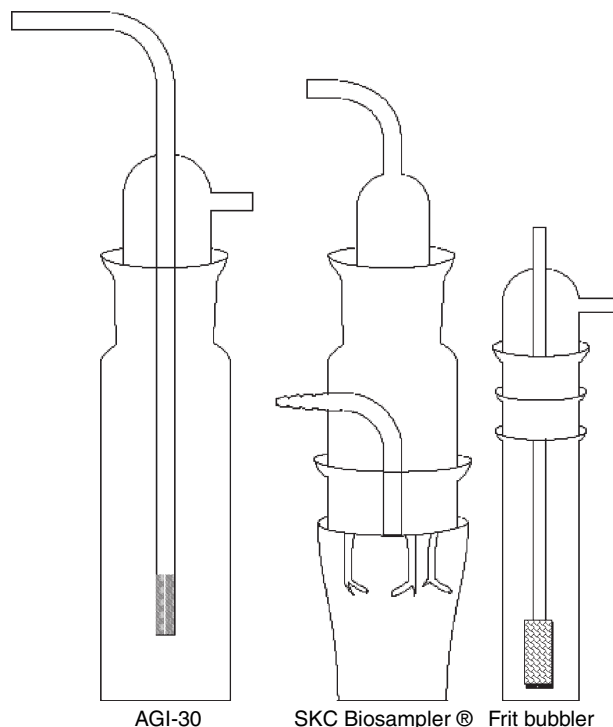


Fig. 1 Drawings of the three liquid-impinging samplers evaluated

surface. Particles with high inertia cannot follow sharp turns in streamlines and will impact and penetrate the liquid surface after exiting the nozzle. The suggested flow rate for the AGI-30 is 12.5 l min^{-1} .

The BioSampler has three 0.630-mm nozzles that are aligned such that flow passing through the nozzles causes a swirling motion in the collection liquid. Like the AGI-30, the recommended operating flow rate of the BioSampler is 12.5 l min^{-1} and it requires 15–20 ml of collecting fluid for operation.

In bubbling aerosol samplers, the aerosol flow creates a bubble in the collecting fluid. The frit bubbler used in this study has a fibrous glass frit where the aerosol contacts the sampling liquid. This porous media device aids in bubble formation and provides a means for interceptional capture of

aerosol particles, where particle transfer to the liquid can occur in the frit region by a complex impaction-type mechanism. Transfer to the liquid could also occur as the particles migrate via diffusion to the air–liquid interface within the bubbles. Because smaller particles have higher diffusion coefficients, collection via diffusion is potentially effective for ultrafine virus particles. While bubblers have been used extensively for the capture of gases, they have rarely been used for the capture of biological particles.

Experimental plan

The experiments performed in this study are listed in Table 1. Five sets of experiments were completed to evaluate the sampler collection efficiency of virus aerosol particles and to determine the number of viable viruses attached to or embedded in particles of a specific size. Similar studies have been conducted to evaluate capture efficiencies of virus aerosol particles by electrical fields (Hogan *et al.* 2004).

Set 1 experiments were performed to determine the size distribution of ultrafine and submicrometre virus aerosols. Aerosols from the previously described MS2 bacteriophage and T3 bacteriophage suspensions were produced by a constant output atomizer operated at an upstream pressure of 240 kPa and a flow rate of 3.5 l min^{-1} . Constant output atomizers, such as the one used in this study, utilize a pressure drop to drive liquid up through a capillary and out of a nozzle, which produces micrometre and submicrometre liquid droplets. The atomizer used in this study also had a built-in impaction plate to remove supermicrometre droplets from the flow stream. It was found that the size distribution of particles generated by the atomizer was not time varying, while particles produced from a collision nebulizer had a time-varying size distribution. Furthermore, the virus titre within the atomizer suspension did not change during 1 h of operation. The suspension droplets the atomizer produced were subsequently dried by passing them through a diffusion dryer (TSI model 3062; TSI, Inc., Minneapolis, MN, USA), leaving submicrometre and ultrafine particles from the suspended and dissolved com-

Table 1 Summary of experiments performed

Set	Purpose	Aerosol	Flow rates (l min^{-1})
1	Measure aerosolized virus particle size distributions	MS2 suspension, T3 suspension	3.5–12.5
2	Measure collection efficiency as a function of Stokes number and particle diameter	MS2 suspension	6.25, 12.5
3	Characterize fluid behaviour of samplers	N/A	0–15
	Measure capture efficiency as a function of flow rate	MS2 suspension	3.5–14.5
4	Measure collection efficiency of viable viruses	MS2 suspension, T3 suspension	12.5
	Measure collection efficiency over time	MS2 suspension	12.5
5	Determine location of viruses in particle size distribution	MS2 suspension, T3 suspension	12.5

ponents of the droplets. Particles were then size classified and counted using a differential mobility analyser (DMA) (TSI model 3081 in Electrostatic Classifier Model 3080) and an ultrafine condensation particle counter (TSI model 3025) operated together as a scanning mobility particle spectrometer (SMPS) (Wang and Flagan 1990). Size distributions, which express the number concentration of particles as a function of particle diameter, were measured in the size range of 9.82–414 nm. Size distributions were measured for aerosol particles produced from suspensions of media both with and without phages present in the suspension.

Set 2 experiments were performed to evaluate the collection efficiency of each sampler as a function of Stokes number and particle diameter d_p (nm). For particles of diameter d_p , the sampler collection efficiency, E_{dp} (%), is defined as:

$$E_{dp} = 100 \left(1 - \frac{N_{dp,out}}{N_{dp,in}} \right), \quad (1)$$

where $N_{dp,out}$ and $N_{dp,in}$ are the number concentration (cm^{-3}) of particles with diameter d_p at the outlet and inlet of the sampler respectively. In inertial samplers such as the ones used in this study, collection efficiency should be a function exclusively of the dimensionless Stokes number (Stk), defined as:

$$\text{Stk} = \frac{\rho_p d_p^2 C_c U_0}{18 \mu d_j}, \quad (2)$$

where ρ_p (kg m^{-3}) is the particle density, U_0 is the velocity at the nozzle exit (m s^{-1}), μ is the gas viscosity (1.82×10^{-5} Pa s for air), and d_j (m) is the nozzle diameter, or characteristic length. C_c is the Cunningham correction factor, or slip correction factor given by:

$$C_c = 1 + \frac{2\lambda}{d_p} \left[1.257 + 0.4 \exp \left(-0.55 \frac{d_p}{\lambda} \right) \right], \quad (3)$$

where λ is the mean free path of air, which is 6.65×10^{-8} m at room temperature and atmospheric pressure (Friedlander 2000). The Stokes number arises from analysis of the drag force a particle experiences as it travels through a fluid medium, and is representative of the particle's inertial penetration distance with respect to a characteristic length (Friedlander 2000). The basic setup used in set 2 experiments is shown in Fig. 2a. Ultrafine and submicrometre particles were produced in an identical manner to set 1 experiments. To adjust the flow rate of particles into the samplers, dry, particle-free dilution air was introduced into the flow stream. Following dilution, the dried particles entered the sampler. Uncollected and reaerosolized particles (emitted from the sampling liquid that were previously collected) exited the tested sampler and passed through a diffusion dryer. Size distributions were measured at the inlet and the outlet of the sampler in order to evaluate collection efficiency. Experiments were run at flow rates of 12.5 and

6.25 l min^{-1} . Both the BioSampler and the AGI-30 were filled with 20 ml of filtered deionized water for sampling, while the bubbler was filled with 10 ml.

Set 3 experiments were performed to characterize the physical behaviour of each sampler as well as the collection efficiency of 25 and 300 nm diameter particles at different operating flow rates. The 25 and 300 nm sizes were chosen to represent the smallest possible virus particles and larger, submicrometre virus particles respectively. The setup for these experiments was the same as the system described previously except that the DMA was operated to select for a fixed particle diameter (25 or 300 nm). The flow rate was varied from 3.5–14.5 l min^{-1} for collection efficiency measurements. Observations were made of sampler liquid behaviour at flow rates of 0–15 l min^{-1} .

In set 4 experiments, sampler collection was evaluated over a period of 1 h. The collection efficiency of each sampler for 25 and 300 nm particles was measured operating each sampler at a flow rate of 12.5 l min^{-1} . In order to determine the number of viable bacteriophages collected in each sampler over time, samplers were filled with 20 ml (10 ml for the frit bubbler) of phosphate-buffered saline solution with a trace amount of Tween-80 and collected virus aerosol particles for 1 h. After periods of 5, 10, 30 and 60 min, sampling liquids were titred using the plaque assay method described by Adams (1959). Samplers were tested with both MS2 and T3 bacteriophage suspensions. Using this measurement, a lower limit on the percentage of viable viruses collected by each sampler was calculated as:

$$E_{LL} = 100 \left(\frac{C_{PFU,s} V_s}{Q_a C_{PFU,a} t} \right), \quad (4)$$

where E_{LL} is the lower limit on the percentage of viruses collected by the sampler, i.e. the total number of viable viruses in the sampler at time t (min) divided by the number of viruses that has entered the sampler in t minutes. $C_{PFU,s}$ and $C_{PFU,a}$ are the virus titres (PFU ml^{-1}) in the sampler at time t and in the atomizer suspension, respectively, Q_a is the liquid flow rate of the atomizer ($0.078 \text{ ml min}^{-1}$) and V_s (ml) is the liquid volume in the sampler at time t . In making this calculation it is assumed that the loss in viability during the atomization process is minimal, thus E_{LL} is a lower limit on the percentage of viable viruses collected.

Set 5 experiments demonstrate a method to determine the size distribution function for particles which contain viable viruses. The system used for these experiments is shown in Fig. 2b. Virus aerosols were created from the atomizer and diffusion dryer, and then passed into the DMA. By fixing the applied potential on the DMA, only particles in a narrow size range can penetrate through the electrostatic classifier. Experiments were run with the DMA applied potential set to voltages corresponding to the penetration of particles in size ranges centred on 25,

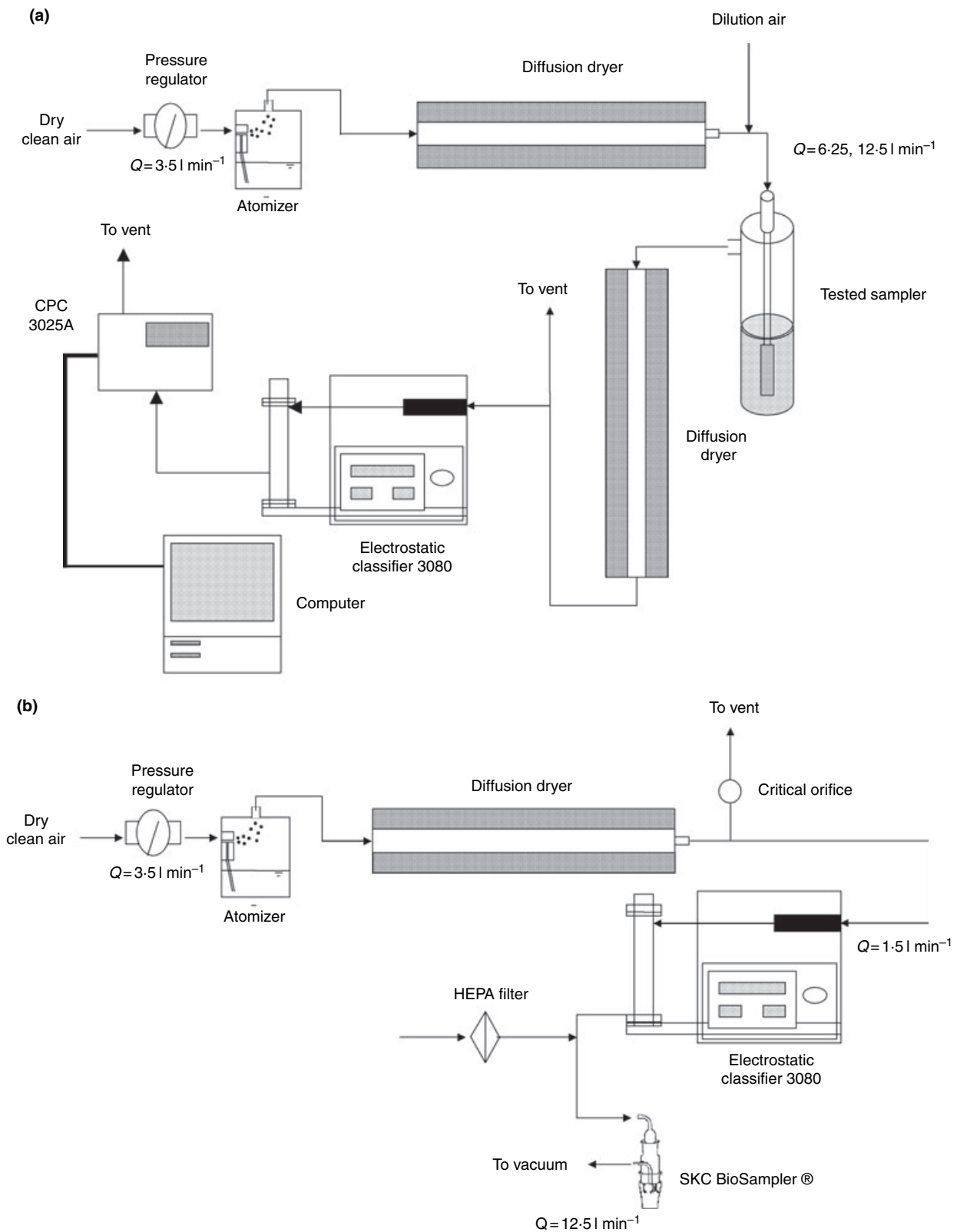


Fig. 2 Schematic diagram of (a) the system used to measure particle size distributions and evaluate sampler collection efficiency and (b) the system used to determine the viable virus particle size distribution function

120 and 300 nm. After exiting the electrostatic classifier, the monodisperse particles entered the BioSampler, which was operated at a flow rate of 12.5 l min^{-1} . To minimize any loss in viability of collected viruses over long sampling times, experiments were conducted for only 30 min. After the 30-min period, the number of collected viruses was measured by performing a plaque assay on the collecting liquid of the BioSampler. Using these data, the viable virus particle size distribution function $\Gamma(d_p)$ (PFU cm^{-3}), was calculated as:

$$\Gamma(d_p) = \frac{1}{E_{dp} P_D Q_D (\Delta \log_{10} d_p)} \frac{C_{\text{PFU},s} V_s}{t}, \quad (5)$$

where Q_D is the flow rate through the DMA (1.5 l min^{-1}), P_D is the penetration of particles of diameter d_p through the DMA (Wiedensohler 1988) and $\Delta \log_{10} d_p$ is logarithm of the width of the DMA transfer function.

RESULTS

The experiments conducted in this study can be divided into five sections: size distribution measurements, collection efficiency measurements, sampling flow rate dependency, virus collection over time, and evaluation of the viable virus size distribution function.

Size distribution of bacteriophage suspensions

The SMPS measured size distributions for atomized MS2 and T3 phage suspensions from set 1 experiments are shown in Fig. 3. Because of the high concentration of small solutes present in virus propagation media, the addition of viruses to the media has little effect on the particle size distribu-

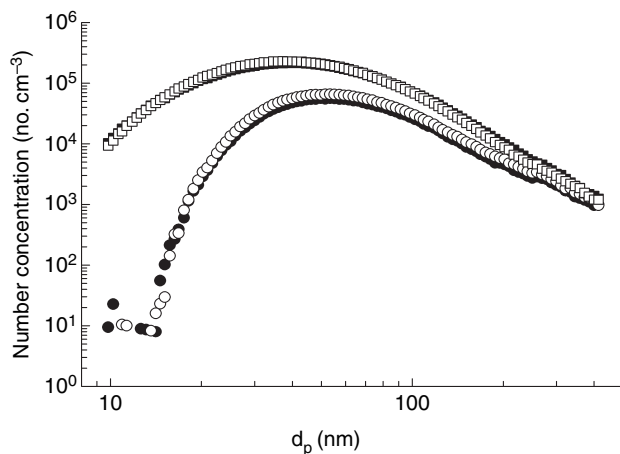


Fig. 3 Size distributions of submicrometre and ultrafine particles produced from the atomization of MS2 and T3 bacteriophage suspensions. ●, MS2 media with phages; ○, MS2 media without phages; ■, T3 media with phages; □, T3 media without phages

tions. To produce aerosol particles, droplets are atomized and dried, leaving behind a high number concentration of residual solute particles. Because such solutes are necessary for the propagation of viruses and maintenance of virus viability, it is difficult to produce aerosol particles where the presence of viruses can be detected by size spectrometric methods from the atomizers and nebulizers traditionally used in aerobiological studies. In general, the size distribution of virus aerosol particles is controlled by the properties of the aerosolized liquid media and the method of aerosolization, not by the physical size of the viruses themselves.

Collection efficiency of liquid based samplers

Figure 4 shows the collection efficiency of each sampler as a function of particle diameter from set 2 experiments. All tested samplers show similar behaviour, with collection increasing with increasing particle diameter for submicrometre particles at a fixed flow rate of 12.5 l min^{-1} . This is presumably because of enhanced impaction and interception collection mechanisms for larger particles. As impactors, all tested samplers have a 50% cutoff diameter of approx. 300 nm, which agrees well with the results of Willeke *et al.* (1998). For particles $<30 \text{ nm}$ in diameter, collection efficiency increases with decreasing particle diameter. Presumably, the mechanism of collection for these ultrafine particles is diffusion, which increases with decreasing particle size. All samplers have a penetration window in the 30–100 nm range where the collection efficiency is approx. 10% or lower. Many viruses have sizes within this range, thus single viruses are typically collected with extremely low efficiency in liquid-based samplers. In order

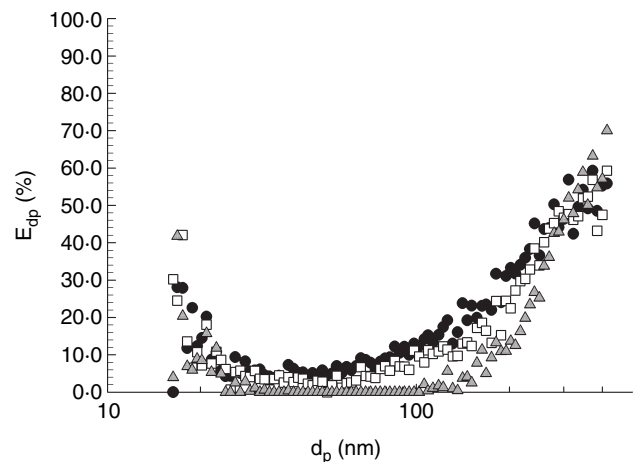


Fig. 4 Collection efficiency as a function of particle diameter with a sampling flow rate of 12.5 l min^{-1} for the (●) All Glass Impinger 30, (□) SKC BioSampler® and (△) frit bubbler. Data shown are the average of five test runs for each sampler

for substantial virus collection in these samplers, viruses must be attached to larger carrier particles.

Figure 5a–c shows the collection efficiency of aerosol particles in (panel a) the AGI-30, (panel b) the SKC BioSampler® and (panel c) the frit bubbler as a function of Stokes number at flow rates of 12.5 and 6.25 l min⁻¹. For impactor-type samplers, it is expected that collection efficiency would be a function of Stokes number (Friedlander 2000), i.e. a change in the flow rate would not change the shape of the collection efficiency vs. Stokes number curve. Clearly, the liquid impingers do not behave as ideal impactors. Several factors could explain the observed curve shifts, such as increased turbulence at higher flow rates. The flow rate dependency is less severe in the frit bubbler, where bubble formation is a function of flow rate but the impacting surface (glass frit) is a nondeformable solid which has flow rate-independent properties.

Sampler behaviour as a function of flow rate

The shift in the Stokes number collection efficiency curves with flow rate led to further investigation of the flow rate dependency in set 3 experiments. A change in sampling liquid behaviour with change in sampler flow rate can be seen visually. At low flow rates, sampling liquids experience little force at the air–liquid interface and the liquid is near motionless. However, as flow rate within a sampler is increased, the force on the liquid can give rise to laminar and turbulent swirling within the AGI-30 and the BioSampler. In the AGI-30, flow rates <1 l min⁻¹ cause minor surface vibrations in the collecting liquid, and no depression in the sampling liquid is evident. For flow rates of 1–2.5 l min⁻¹, a small depression forms within the liquid directly below the nozzle outlet of the impinger. As flow rate is increased beyond 2.5 l min⁻¹, the liquid surface is disrupted, resulting in turbulent liquid motion. Turbulence increases with increasing flow rate for all allowable operational flow rates within the AGI-30. In the BioSampler, the sampling liquid remains motionless within a flow rate range of 0–2.5 l min⁻¹. Minor surface vibrations occur for flow rates of 2.5–4 l min⁻¹. Beyond 4 l min⁻¹, and up to approx. 8.7 l min⁻¹, the sampling liquid swirls in a laminar fashion, driven by the flow of the BioSampler's three angled nozzles. A visual laminar to turbulent transition occurs in the sampling liquid for aerosol flow rates above 8.7 l min⁻¹, and liquid behaviour is increasingly turbulent as the flow rate increases beyond 8.7 l min⁻¹. While no transitional regimes are apparent for bubbler liquid behaviour, changes in flow rate can also change bubble formation rate, size distribution and velocity distribution within the bubbler. Bubble formation was possible at all tested flow rates. It must be noted that the transitional flow rates described here apply when water is

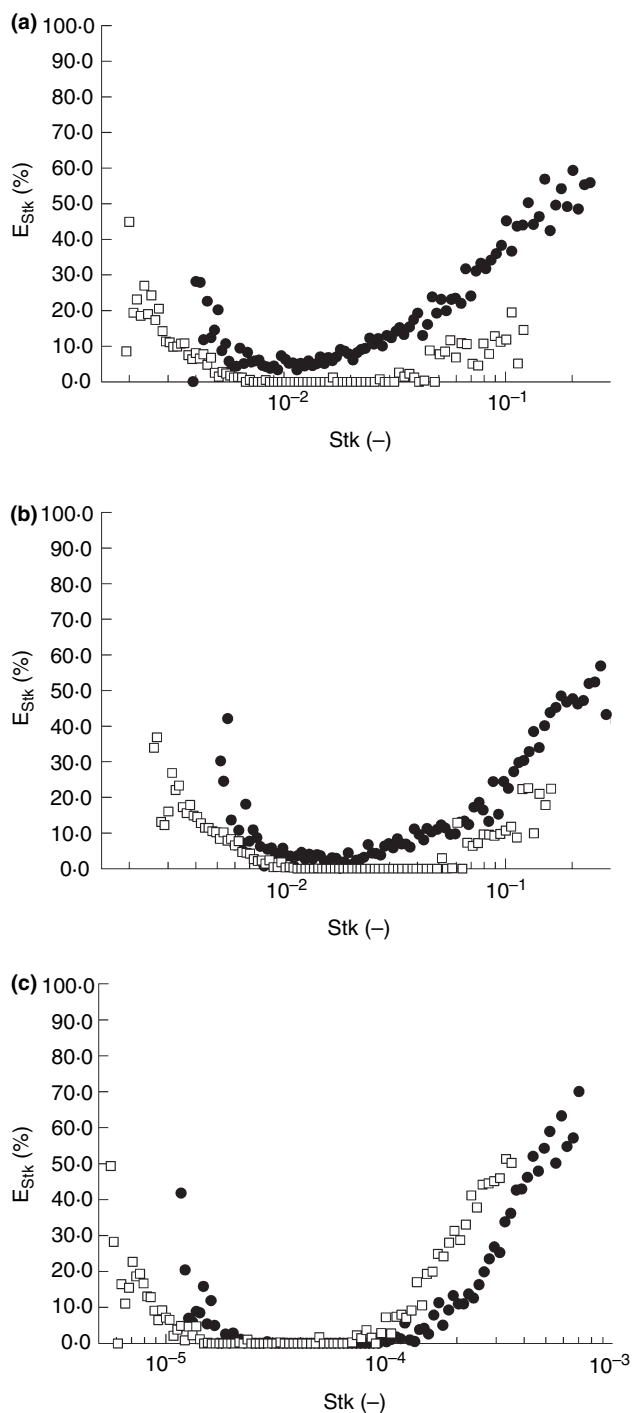


Fig. 5 Collection efficiency as function of Stokes number for the (a) All Glass Impinger-30, (b) SKC BioSampler®, and (c) frit bubbler with sampling flow rates of (●) 12.5 l min⁻¹ and (□) 6.25 l min⁻¹. Data shown are the average of five test runs for each sampler

used as the sampling liquid. The flow rate at which such transitions occur is highly dependent upon the viscosity and density of the sampling liquid.

Figure 6 shows the collection efficiency as a function of flow rate for 25 and 300 nm particles. For all flow rates, the collection efficiency of 25 nm particles in all samplers is below 25%. In the AGI-30 and SKC BioSampler, 25 nm collection decreases with increasing flow rate at low flow rates, then increases with increasing flow rate at higher flow rates. Presumably, at low flow rates, 25 nm particles are captured by Brownian motion; thus increasing the flow rate decreases collection efficiency due to the decrease in residence time within the sampler. However, as flow rate increases in these samplers and the flow undergoes a turbulent transition (as seen in visual observations), the collection mechanism changes from Brownian motion to turbulent diffusion or dispersion. In the frit bubbler, there is no such U-shaped collection efficiency vs. flow rate relationship for 25 nm particles, presumably because they are not adequately captured by diffusion mechanisms within

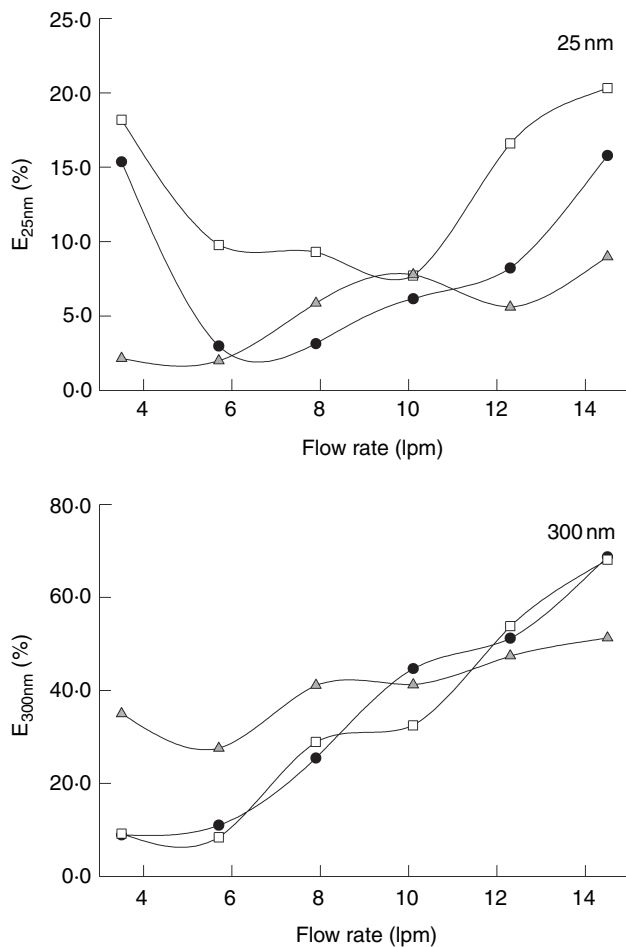


Fig. 6 Collection efficiency as a function of flow rate using 25 nm particles and 300 nm particles for the (●) All Glass Impinger 30, (□) SKC BioSampler® and (△) frit bubbler. Data shown are the average of five tests for each sampler

the bubbler. For all samplers, 300 nm particle collection efficiency increases almost linearly with flow rate. Because the inertial collection of the SKC BioSampler® was designed to mimic the inertial collection of the AGI-30 (Willeke *et al.* 1998), the two samplers have near identical collection efficiency vs. flow rate curves for particles collected by impaction.

Virus collection over time

Set 4 experiments investigated virus collection over time. All samplers lost sampling liquid as a result of evaporation and aerosolization at a rate of approx. 0.1 ml min^{-1} . Figure 7 shows the collection efficiency of 25 and 300 nm particles over a 1-h sampling period in all three tested samplers. In both the AGI-30 and SKC BioSampler, collection efficiency of both 25 and 300 nm particles slowly decreases with time, likely because of evaporative losses and aerosolization of sampling liquid. In the frit bubbler, however, collection

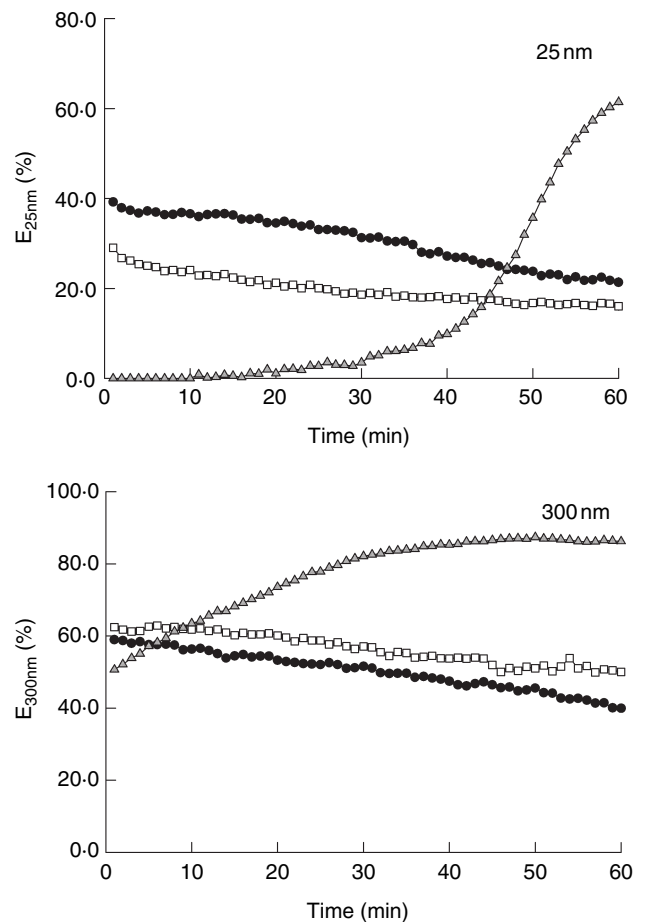


Fig. 7 Representative collection efficiency curves as a function of time using 25 and 300 nm particles for the (●) All Glass Impinger 30, (□) SKC BioSampler® and (△) frit bubbler

efficiency rapidly increases over time for 300 nm particles. Collection efficiency is low for 25 nm particles for the initial 30 min of sampling, then sharply increases. This could be explained by the deposition of particles within the glass frit over time increasing the efficiency of particle capture by interception. Larger particles would immediately experience increased capture by interception, while the effect would be delayed on smaller particles, which would not be able to be captured until significant particle deposition had occurred on the frit. The improved collection efficiency over time could also be related to the reduced aerosolization from bubbler (Deppert *et al.* 1994; Deppert and Wiedensohler 1994) which would also effectively increase measured collection efficiency.

The virus titres in the sampling liquid for MS2 and T3 bacteriophage aerosols are shown in Fig. 8a. For both MS2 and T3 bacteriophages, the SKC BioSampler® shows the lowest but the most linear collection with time, with the

exception of after 10 min of collection where the BioSampler has a slightly decreased collected phage titre for both test viruses. The AGI-30 shows consistent collection for T3 bacteriophages, however MS2 phages appear to lose viability within the AGI-30 after a sampling period of 30 min, indicated by the large decrease in the phage titre in the sampling liquid between 30 and 60 min sampling periods. Similar to the time-based collection efficiency measurements, the frit bubbler shows an increase in phage collection with time, as seen by the concave shape of the concentration vs. sampling time curve. This sampling behaviour is the result of both the increased collection efficiency with time within the frit bubbler, as well as large sampler volume losses (up to 70% of the sampling liquid) increasing the virus titre with time. The AGI-30 and BioSampler also show some degree of concave behaviour, which would not be expected based on physical measurements of collection efficiency over time. This is in part due to the fact that, like

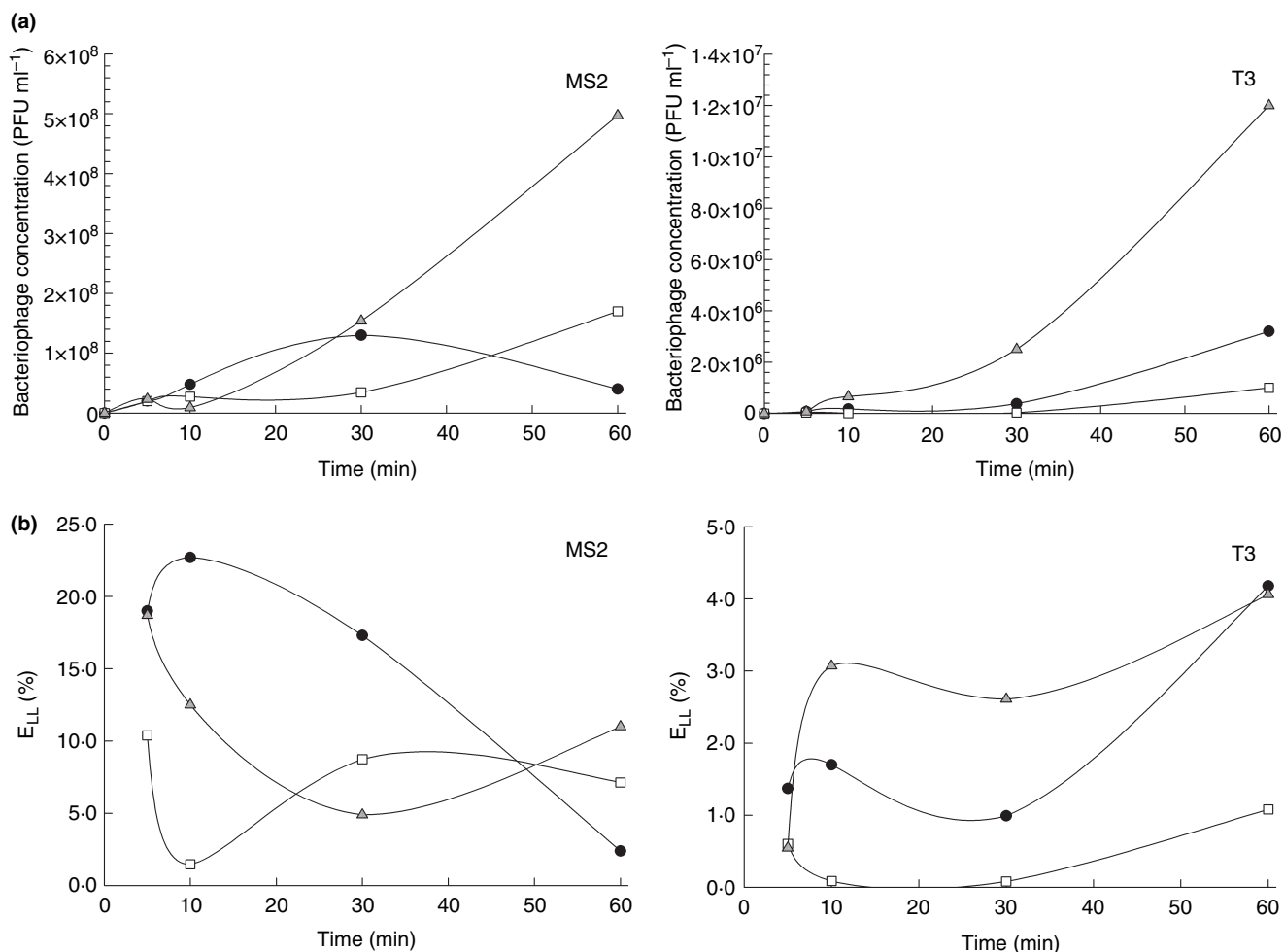


Fig. 8 (a) Representative sampling liquid virus titres and (b) the lower limit on the fraction of viruses collected, E_{LL} , over time using MS2 bacteriophages and T3 bacteriophages for the (●) All Glass Impinger 30, (□) SKC BioSampler® and (△) frit bubbler

the frit bubbler, the AGI-30 and BioSampler lose sampling liquid over time. However, losses in sampling liquid alone are not adequate to account for the nonlinear behaviour of virus collection over time, and therefore this behaviour must be related to transient losses in collected virus viability.

Measurement of E_{LL} , shown in Fig. 8b, can provide more insight into the nonlinear behaviour of samplers as virus collectors. For an ideal sampler, which has constant collection efficiency and maintains virus viability during sample, E_{LL} should be constant for all sampling times. For all samplers, E_{LL} is highly variable, indicating the samplers are very nonconstant in terms of collecting virus particles and maintaining the viability of collected viruses.

Viable virus particle size distribution

In determining the viable virus particle size distribution function, $\Gamma(d_p)$, the BioSampler was used because it was determined that it had the most constant E_{LL} for a 30-min sampling period. Figure 9 shows the eqn (5) calculated

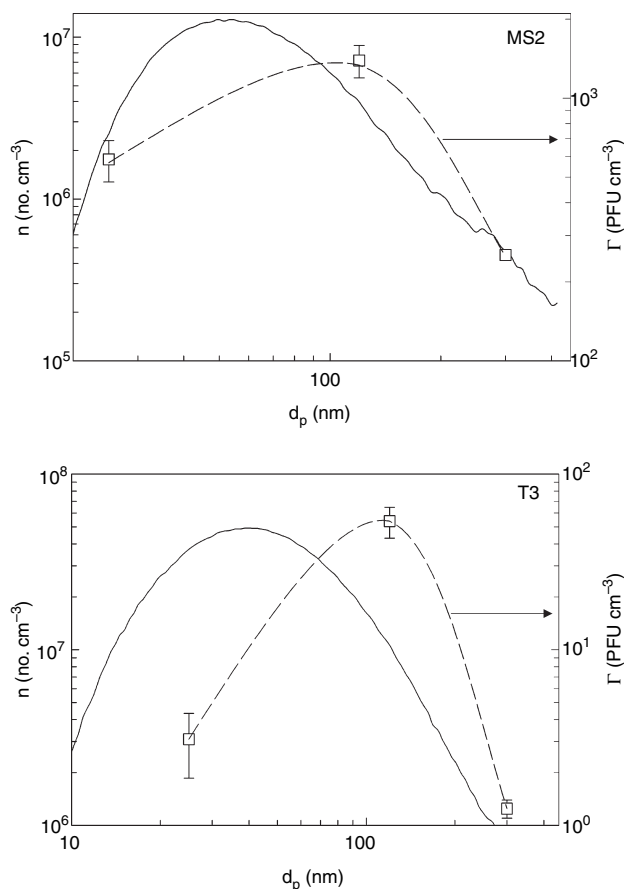


Fig. 9 Size distribution functions for all particles and viable virus particles using MS2 bacteriophages and T3 bacteriophages. Errors bars indicate the standard deviation of three tests

$\Gamma(d_p)$ values at particle diameters of 25, 120 and 300 nm for both atomized MS2 and T3 phage suspensions. Also shown is the size distribution function of all aerosol particles produced by the atomizer, $n(d_p)$ (Friedlander 2000). The presence of virus particles at 25 nm from the MS2 suspension implies that despite the presence of a high concentration of particle forming small solutes, some virus particles do exist as single viruses in the air. The detection of an extremely small number of viable T3 viruses in 25 nm particles is presumably the result of highly charged larger particles passing through the DMA with the same electrical mobility as a singly charged 25 nm particle, as T3 viruses are larger than 25 nm in diameter. For both MS2 and T3 bacteriophage aerosols, the size distribution function of the total particles is greater than the size distribution function of the viable virus particles by several orders of magnitude. This implies that the addition of viruses to suspensions for aerosolization will have little effect on the resulting size distribution, which is dominated by the presence of particle forming solute molecules, and that the probability of an individual particle containing more than one viable virus is extremely low. Compared with the total particle size distribution functions, the viable virus particle size distribution functions are shifted to the right. If airborne virus viability is not effected by the size of virus carrier particle, this trend would be expected because larger particles have a higher probability of containing a virus particle. By taking the ratio of the viable virus size distribution function to the total particle size distribution function at the three measured sizes, it can be seen that larger particles from the MS2 phage suspension have a higher probability of containing a viable virus particle. However, this is not the case for the T3 suspension, where the viable virus size distribution decreases sharply from 120 to 300 nm. This implies that T3 bacteriophages lose viability when embedded in larger, dried particles. Because of the low number of larger particles in virus size distributions, most of the virus particles in both the atomized MS2 and T3 phage suspensions reside on or within particles <300 nm in diameter. Thus, liquid impingement samplers will have extremely low collection efficiencies for virus containing particles which are produced by similar atomization and nebulization techniques.

DISCUSSION

The methods and data shown here give a full-scale evaluation of virus atomization techniques and virus aerosol particle collection by liquid impingement. Similar aerosolization and collection methods have been used in the study of factors affecting the viability of airborne viruses (Trouwborst *et al.* 1972; Trouwborst and de Jong 1973; Trouwborst and Kuyper 1974; Sattar *et al.* 1984; Ijaz *et al.* 1994; Tseng and Li 2005); however, issues with physical collection efficiency

have not been addressed. Because viruses are typically in relatively low concentration compared with the medium in which they are present, their presence has no effect on the size distribution resulting from the aerosolization of the virus-containing medium. Several researchers have made attempts to circumvent this issue by changing suspension properties and using novel aerosolization methods. Hogan *et al.* (2004) nebulized and atomized suspensions of freeze-dried MS2 bacteriophage particles which had low concentrations of small solutes but contained milk proteins and other organic molecules necessary for virus preservation. To produce single virus particles without any residual solute particles, several researchers have used charge-reduced electrospray systems (Bacher *et al.* 2001; Kuzmanovic *et al.* 2003; Thomas *et al.* 2004). Research is currently underway in our laboratory to study the characteristics of single virus aerosol particles produced by the electrospray technique.

While the presence of airborne viruses is difficult to determine by size spectrometric methods, control over the size distribution of virus-containing particles is possible. By controlling the solute concentrations and virus titres in atomized suspensions, aerosol particles of a controlled size and infectivity can be generated, as particle size is independent of virus size and titre. This would be very useful in targeting virus deposition in different areas of the respiratory system during virus respiratory challenges (Wolff and Dorato 1993; Roy and Hartings 2003).

The samplers used in this study have several problems in the sampling of virus aerosol particles, namely low collection efficiency in particle size ranges of interest, time-varying collection efficiency, and potential for loss of virus viability during collection. Other samplers which utilize liquid impingement, such as the All Glass Impinger 4 (ACE Glass), can be expected to behave in a similar manner. Careful measurements need to be made on such samplers in order to effectively use them to calculate virus concentrations in ambient sampling studies or in the calculation of dosage during respiratory challenges (Dorato and Wolff 1991; Wolff and Dorato 1993; Bray *et al.* 2002; Cassee *et al.* 2002; Esmen *et al.* 2002). The method developed in this study to determine E_{LL} can be applied to any sampler for the collection of any virus in order to determine a correction factor for dosage calculation, assuming the viable virus particle size distribution function used in calibration is identical to that entering the sampler during experimentation. E_{LL} calculation (see eqn 4) does not require any instrumentation beyond that which is necessary for normal sampler operation and measurement; the only necessary parameters are the total number of viruses aerosolized and the total number of viruses collected, both in a given amount of time. Furthermore, E_{LL} calculation is not only applicable to submicrometre and ultrafine particles, but also larger

particles, as the method to calculate it does not utilize any size classification techniques.

Several alternative sampling methods could be used to increase the collection efficiency of virus samplers, such as a bubbling filter sampler (Agranovski *et al.* 1999, 2004a,b) and an aerosol concentration system where particles are grown by a condensation process to a collectable size (Kim *et al.* 2001a,b). Electrical methods, which have been applied to the collection of bacterial aerosol particles (Mainelis *et al.* 1999, 2002a,b), would also offer increased collection efficiency for ultrafine and submicrometre virus particles (Hogan *et al.* 2004). While improved sampling systems can increase the collection efficiency of samplers to allow for high collection of submicrometre and ultrafine particles, virus viability during collection remains an issue. The experiments conducted here, as well as previous research (Trouwborst and de Jong 1972, 1973; Trouwborst and Kuyper 1974; Agranovski *et al.* 2004a,b; Tseng and Li 2005) suggest that virus viability during sampling must be taken into account by testing viruses individually, i.e. very few generalizations can be made for the viability of viruses during airborne sampling. Therefore, the assessment of airborne virus threats by experimentation with surrogate virus particles may not accurately represent the behaviour of infectious airborne viruses in terms of virus viability and stability while in the aerosol phase.

In both ambient virus sampling studies and in animal respiratory challenges, the main goal of sampling is to correctly determine the airborne virus concentration, and to also determine the size of virus particles. Particle size is the key component in determining where a particle will deposit in the lungs, thus equal virus or drug dosages administered from different size aerosol particles will have different toxicological and immunological effects (Cassee *et al.* 2002; Esmen *et al.* 2002; Roy *et al.* 2003b). The method described and applied here utilizing differential mobility analysis for particle size selection and subsequent collection of monodisperse virus particles can be readily used to determine the size distribution function of viable virus particles. This method can be used in conjunction with a wide variety of biological techniques in order to assess the chemical composition and biological effects of aerosol particles as a function of particle size. For rigorous inhaled dosage calculations, parameters such as Γ presented here are necessary and should be used in future inhalation studies.

ACKNOWLEDGEMENTS

This work was partially supported by the Midwest Regional Center of Excellence (MRCE) for Biodefense and Emerging Infectious Disease Research Developmental Project Grant funded by the National Institute of Health.

REFERENCES

- Adams, M.H. (1959) *Bacteriophages*. pp. 450–456. New York: Interscience Publishers Inc.
- Agranovski, I.E., Braddock, R.D. and Myojo, T. (1999) Removal of aerosols by bubbling through porous media. *Aerosol Sci Tech* **31**, 249–257.
- Agranovski, I.E., Agranovski, V., Reponen, T., Willeke, K. and Grinshpun, S.A. (2002) Development and evaluation of a new personal sampler for culturable airborne microorganisms. *Atmos Environ* **36**, 889–898.
- Agranovski, I.E., Safatov, A.S., Borodulin, A.I., Pyankov, O.V., Petrishchenko, V.A., Sergeev, A.N., Agafonov, A.P., Ignatiev, O.N. *et al.* (2004a) Inactivation of viruses in bubbling processes utilized for personal bioaerosol monitoring. *Appl Environ Microbiol* **70**, 6963–6967.
- Agranovski, I.E., Safatov, A.S., Pyankov, O.V., Sergeev, A.N., Agafonov, A.P., Ignatiev, G.M. *et al.* (2004b) Monitoring of viable airborne SARS virus in ambient air. *Atmos Environ* **38**, 3879–3884.
- Aller, J.Y., Kuznetsova, M.R., Jahns, C.J. and Kemp, P.F. (2005) The seas surface microlayer as a source of viral and bacterial enrichment in marine aerosols. *J Aerosol Sci* **36**, 801–812.
- Bacher, G., Szymanski, W.W., Kaufman, S.L., Zollner, P., Blaas, D. and Allmaier, G. (2001) Charge-reduced nano electrospray ionization combined with differential mobility analysis of peptides, proteins, glycoproteins, noncovalent protein complexes and viruses. *J Mass Spectrom* **36**, 1038–1052.
- Bray, M., Martinez, M., Kefauver, D., West, M. and Roy, C. (2002) Treatment of aerosolized cowpox virus infection in mice with aerosolized cidofovir. *Antiviral Res* **54**, 129–142.
- Brooks, J.P., Tanner, B.D., Gerba, C.P., Haas, C.N. and Pepper, I.L. (2005) Estimation of bioaerosol risk of infection to residents adjacent to a land applied biosolids site using an empirically derived transport model. *J Appl Microbiol* **98**, 397–405.
- Cassee, F.R., Muijser, H., Duistermaat, E., Freijer, J.J., Geerse, K.B., Marijnissen, J.C.M. and Arts, J.H.E. (2002) Particle size-dependent total mass deposition in lungs determines inhalation toxicity of cadmium chloride aerosols in rats. Application of a multiple path dosimetry model. *Arch Toxicol* **76**, 277–286.
- Daigle, C.C., Chalupa, D.C., Gibb, F.R., Morrow, P.E., Oberdorster, G., Utell, M.J. and Frampton, M.W. (2003) Ultrafine particle deposition in humans during rest and exercise. *Inhal Toxicol* **15**, 539–552.
- Deppert, K. and Wiedensohler, A. (1994) Aerosol-particles from bubblers in metalorganic vapor-phase epitaxy. *Crystal Res Tech* **29**, 613–616.
- Deppert, K., Hansson, H.C., Jeppesen, S., Miller, M.S., Samuelson, L., Seifert, W. and Wiedensohler, A. (1994) Aerosol-particles from metalorganic vapor-phase epitaxy bubblers. *J Crystal Growth* **145**, 636–641.
- Dorato, M.A. and Wolff, R.K. (1991) Inhalation exposure technology, dosimetry, and regulatory issues. *Toxicol Pathol* **19**, 373–383.
- Esmen, N.A., Johnson, D.L. and Agron, G.M. (2002) The variability of delivered dose of aerosols with the same respirable concentration but different size distributions. *Ann Occup Hyg* **46**, 401–407.
- Friedlander, S.K. (2000) *Smoke, Dust, and Haze*. New York: Oxford University Press.
- Golmohammadi, R., Valegard, K., Fridborg, K. and Liljas, L. (1993) The refined structure of bacteriophage-MS2 at 2.8 Angstrom resolution. *J Mol Biol* **234**, 620–639.
- Grinshpun, S.A., Willeke, K., Ulevicius, V., Juozaitis, A., Terzieva, S., Donnelly, J. *et al.* (1997) Effect of impaction, bounce and reaerosolization on the collection efficiency of impingers. *Aerosol Sci Tech* **26**, 326–342.
- Hirst, G.K. and Pons, M.W. (1973) Mechanism of influenza recombination. II. Virus aggregation and its effect on plaque formation by so-called noninfective virus. *Virology* **56**, 620–631.
- Hogan, C.J., Lee, M.-H. and Biswas, P. (2004) Capture of viral particles in soft X-ray-enhanced corona systems: charge distribution and transport characteristics. *Aerosol Sci Tech* **38**, 475–486.
- Hull, R., Hills, G.J. and Plaskitt, A. (1970) The in vivo behaviour of twenty-four strains of alfalfa mosaic virus. *Virology* **42**, 753–772.
- Ijaz, M.K., Sattar, S.A., Alkarmi, T., Dar, F.K., Bhatti, A.R. and Elhag, K.M. (1994) Studies on the survival of aerosolized bovine rotavirus (Uk) and a murine rotavirus. *Comp Immunol Microbiol Infect Dis* **17**, 91–98.
- Kim, S., Jaques, P.A., Chang, M.C., Froines, J.R. and Sioutas, C. (2001a) Versatile aerosol concentration enrichment system (VACES) for simultaneous in vivo and in vitro evaluation of toxic effects of ultrafine, fine and coarse ambient particles – Part I: development and laboratory characterization. *J Aerosol Sci* **32**, 1281–1297.
- Kim, S., Jaques, P.A., Chang, M.C., Barone, T., Xiong, C., Friedlander, S.K. and Sioutas, C. (2001b) Versatile aerosol concentration enrichment system (VACES) for simultaneous in vivo and in vitro evaluation of toxic effects of ultrafine, fine and coarse ambient particles – Part II: field evaluation. *J Aerosol Sci* **32**, 1299–1314.
- Kuzmanovic, D.A., Elashvili, I., Wick, C., O'Connell, C. and Krueger, S. (2003) Bacteriophage MS2: molecular weight and spatial distribution of the protein and RNA components by small-angle neutron scattering and virus counting. *Structure* **11**, 1339–1348.
- Lin, X.J., Willeke, K., Ulevicius, V. and Grinshpun, S.A. (1997) Effect of sampling time on the collection efficiency of all-glass impingers. *Am Ind Hyg Assoc J* **58**, 480–488.
- Lin, X.J., Reponen, T.A., Willeke, K., Grinshpun, S.A., Foarde, K.K. and Ensor, D.S. (1999) Long-term sampling of airborne bacteria and fungi into a non-evaporating liquid. *Atmos Environ* **33**, 4291–4298.
- Lin, X.J., Reponen, T., Willeke, K., Wang, Z., Grinshpun, S.A. and Trunov, M. (2000) Survival of airborne microorganisms during swirling aerosol collection. *Aerosol Sci Tech* **32**, 184–196.
- Madigan, M.T., Martinko, J.M. and Parker, J. (1997) *Biology of Microorganisms*. Upper Saddle River, NJ: Prentice Hall.
- Mainelis, G., Grinshpun, S.A., Willeke, K., Reponen, T., Ulevicius, V. and Hintz, P.J. (1999) Collection of airborne microorganisms by electrostatic precipitation. *Aerosol Sci Tech* **30**, 127–144.
- Mainelis, G., Willeke, K., Adhikari, A., Reponen, T. and Grinshpun, S.A. (2002a) Design and collection efficiency of a new electrostatic precipitator for bioaerosol collection. *Aerosol Sci Tech* **36**, 1073–1085.
- Mainelis, G., Adhikari, A., Willeke, K., Lee, S.A., Reponen, T. and Grinshpun, S.A. (2002b) Collection of airborne microorganisms by a new electrostatic precipitator. *J Aerosol Sci* **33**, 1417–1432.
- Roy, C.J. and Hartings, J.M. (2003) An automated aerosol system that uses real-time dosimetry for inhalation exposures with primates. *Toxicol Sci* **72**, 296.

- Roy, C.J., Baker, R., Washburn, K. and Bray, M. (2003a) Aerosolized cidofovir is retained in the respiratory tract and protects mice against intranasal cowpox virus challenge. *Antimicrob Agents Chemother* **47**, 2933–2937.
- Roy, C.J., Hale, M., Hartings, J.M., Pitt, L. and Duniho, S. (2003b) Impact of inhalation exposure modality and particle size on the respiratory deposition of ricin in balb/c mice. *Inhal Toxicol* **15**, 619–638.
- Sattar, S.A., Ijaz, M.K., Johnson-Lussenburg, C.M. and Springthorpe, V.S. (1984) Effect of relative humidity on the airborne survival of rotavirus SA11. *Appl Environ Microbiol* **47**, 879–881.
- Terzieva, S., Donnelly, J., Ulevicius, V., Grinshpun, S.A., Willeke, K., Stelma, G.N. and Brenner, K.P. (1996) Comparison of methods for detection and enumeration of airborne microorganisms collected by liquid impingement. *Appl Environ Microbiol* **62**, 2264–2272.
- Thomas, J.J., Bothner, B., Traina, J., Benner, W.H. and Siuzdak, G. (2004) Electrospray ion mobility spectrometry of intact viruses. *Spectroscopy* **18**, 31–36.
- Trouwborst, T. and de Jong, J.C. (1972) Mechanism of the inactivation of the bacteriophage T1 in aerosols. *Appl Microbiol* **23**, 938–941.
- Trouwborst, T. and de Jong, J.C. (1973) Interaction of some factors in the mechanism of inactivation of bacteriophage MS2 in aerosols. *Appl Microbiol* **26**, 252–257.
- Trouwborst, T. and Kuyper, S. (1974) Inactivation of bacteriophage T3 in aerosols: effect of prehumidification on survival after spraying from solutions of salt, peptone, and saliva. *Appl Microbiol* **27**, 834–837.
- Trouwborst, T., de Jong, J.C. and Winkler, K.C. (1972) Mechanism of inactivation in aerosols of bacteriophage T1. *J Gen Virol* **15**, 235–242.
- Trouwborst, T., Kuyper, S. and Teppema, J.S. (1974) Structural damage of bacteriophage T1 by surface inactivation. *J Gen Virol* **25**, 75–81.
- Tseng, C.C. and Li, C.S. (2005) Collection efficiencies for aerosol samplers for virus-containing aerosols. *J Aerosol Sci* **36**, 593–607.
- Wang, S.C. and Flagan, R.C. (1990) Scanning electrical mobility spectrometer. *Aerosol Sci Tech* **13**, 230–240.
- Wiedensohler, A. (1988) An approximation of the bipolar charge-distribution for particles in the sub-micron size range. *J Aerosol Sci* **19**, 387–389.
- Willeke, K., Lin, X.J. and Grinshpun, S.A. (1998) Improved aerosol collection by combined impaction and centrifugal motion. *Aerosol Sci Tech* **28**, 439–456.
- Wolff, R.K. and Dorato, M.A. (1993) Toxicologic testing of inhaled pharmaceutical aerosols. *Crit Rev Toxicol* **23**, 343–369.